

MDPI

Article

# Orthogonal Frequency Division Diversity and Multiplexing for 6G OWC: Principle and Underwater Use Case

Jiamin Chen <sup>1</sup>, Chen Chen <sup>1,\*</sup>, Zhihong Zeng <sup>1</sup>, Min Liu <sup>1</sup>, Jia Ye <sup>2</sup>, Cuiwei He <sup>3</sup>, Shenjie Huang <sup>4</sup>, H. Y. Fu <sup>5</sup> and Harald Haas <sup>6</sup>

- School of Microelectronics and Communication Engineering, Chongqing University, Chongqing 400044, China; 202212021081t@stu.cqu.edu.cn (J.C.); zhihong.zeng@cqu.edu.cn (Z.Z.); liumin@cqu.edu.cn (M.L.)
- <sup>2</sup> School of Electrical Engineering, Chongqing University, Chongqing 400044, China; jia.ye@cqu.edu.cn
- School of Information Science, Japan Advanced Institute of Science and Technology, Ishikawa 923-1211, Japan; cuiweihe@jaist.ac.jp
- School of Engineering, The University of Edinburgh, Edinburgh EH9 3JL, UK; shenjie.huang@ed.ac.uk
- Tsinghua Shenzhen International Graduate School, Tsinghua University, Shenzhen 518055, China; hyfu@sz.tsinghua.edu.cn
- Department of Engineering, University of Cambridge, Cambridge CB3 0FA, UK; huh21@cam.ac.uk
- \* Correspondence: c.chen@cqu.edu.cn

**Abstract:** In this paper, we, for the first time, propose and demonstrate an orthogonal frequency division diversity and multiplexing (OFDDM) scheme for the sixth-generation (6G) underwater optical wireless communication (UOWC) systems. In OFDDM, the subcarriers are grouped into subblocks; the subcarriers within each subblock transmit the same constellation symbol through diversity transmission, while different subblocks transmit different constellation symbols via multiplexing transmission. As a result, OFDDM can support hybrid diversity and multiplexing transmission simultaneously. Moreover, the combination of subblock interleaving and low-complexity diversity is further proposed to efficiently mitigate the adverse low-pass effect and substantially reduce the computational complexity, respectively. The feasibility of OFDDM adapting to the various transmission conditions in UOWC systems has been verified via both simulations and experiments. Experimental results demonstrate that a striking 106.1% effective bandwidth extension can be obtained using OFDDM in comparison to conventional orthogonal frequency division multiplexing (OFDM) for a fixed spectral efficiency of 1 bit/s/Hz. Furthermore, OFDDM with adaptive bit loading can also gain a remarkable 13.3% capacity improvement compared with conventional OFDM with adaptive bit loading.

Keywords: visible light communication; rate splitting; generalized multiple access



Citation: Chen, J.; Chen, C.; Zeng, Z.; Liu, M.; Ye, J.; He, C.; Huang, S.; Fu, H.; Haas, H.Y. Orthogonal Frequency Division Diversity and Multiplexing (OFDDM) for 6G OWC: Principle and Underwater Use Case. *Photonics* 2024, 11, 1051. https://doi.org/10.3390/ photonics11111051

Received: 14 October 2024 Revised: 5 November 2024 Accepted: 7 November 2024 Published: 8 November 2024



Copyright: © 2024 by the authors. Licensee MDPI, Basel, Switzerland. This article is an open access article distributed under the terms and conditions of the Creative Commons Attribution (CC BY) license (https://creativecommons.org/licenses/by/4.0/).

# 1. Introduction

With the rapid development of the communication industry, researchers have commenced exploration of sixth-generation (6G) wireless communication systems [1]. Sixth-generation wireless networks are expected to meet the high data rate and low latency requirements of a variety of applications [2]. Specifically, 6G will support underwater and space communications to significantly expand the boundaries of human activity [3]. In recent years, with the ever-growing global climate change and resource depletion, the ocean has attracted increasing research interests due to its abundant biological, petroleum, and mineral resources [4]. Increasingly frequent underwater activities require large-bandwidth and high-capacity underwater communications between underwater devices [5]. Underwater communications can generally categorized into underwater wired communications and underwater wireless communications. Underwater wired communication is achieved by laying submarine cables. However, the deployment and maintenance of a wired underwater communication system is a time-consuming and labor-intensive task due to the vast area of the ocean [6]. Therefore, underwater wireless communication is a practical solution

Photonics **2024**, 11, 1051 2 of 18

for underwater communication, which consists of radio frequency (RF) communication, acoustic communication and optical wireless communication (OWC). Considering the severe attenuation of RF waves and the drawbacks of acoustic communication such as a low data rate and high latency, underwater OWC (UOWC) has become a potential alternative since it can provide a higher data rate and a lower transmission latency [7–10].

Despite the advantages of UOWC, it still faces challenges such as imperfect transceiver alignment and turbulence [11]. In particular, the received optical power will be greatly reduced, and the received signal-to-noise ratio (SNR) will fluctuate with time due to the random movements of transceivers, and it is found that the turbulence-induced signal fading considerably increases the average bit error rate (BER) of the UOWC system [12]. Furthermore, practical UOWC systems are generally bandlimited and exhibit a typical low-pass characteristic, due to the low-pass nature of the adopted optical components such as light-emitting diodes (LEDs), laser diodes (LDs), and photo-detectors (PDs). Therefore, it is very urgent and of practical significance to develop new techniques in order to enhance the performance of bandlimited UOWC systems under dynamic and complex underwater environments.

## 1.1. Related Work and Motivation

Up to now, many techniques have been reported to improve the performance of practical bandlimited UOWC systems in the literature. More precisely, two major focuses for improving the performance of bandlimited UOWC systems are BER and capacity. In terms of the BER of UOWC systems, error correction coding is a prominent approach to overcome the attenuation from scattering and absorption in underwater environments [13]. Particularly, Hamming code is the simplest linear code that can be easily implemented with low complexity; however, it cannot resolve multi-bit errors, and it has relatively low fault tolerance [14,15]. In [16], the performance of low-density parity-check codes, convolution codes, and turbo codes was compared. Additionally, Reed Solomon codes were utilized to alleviate fading concerns in [17]. In [18,19], pairwise coding (PWC) was designed to mitigate the SNR imbalance due to the low-pass band limitations. In terms of the capacity of UOWC systems, pre- or post-equalization techniques were widely used to directly extend the usable bandwidth of the bandlimited UOWC system [20–22]. However, to successfully perform pre-equalization, channel information feedback is usually needed, which unavoidably reduces the achievable data rate and increases the overall implementation complexity. In addition, pre-equalization may be susceptible to LED/LD nonlinearity when the low-pass effect is relatively severe [23]. Furthermore, post-equalization usually has relatively high computational complexity, which might limit its application in many practical UOWC scenarios.

In addition to the coding schemes and pre- or post-equalization techniques, the adopted modulation scheme also largely affects the performance of intensity modulation/direct detection (IM/DD)-based UOWC systems. So far, on-off keying (OOK) and pulse position modulation (PPM) have been frequently utilized in UOWC systems due to the ease of implementation and low power consumption [24]. In spite of the simplicity, adaptive detection is generally needed for OOK to achieve satisfactory performance, while PPM usually requires the use of a very tight pulse and the process of accurate symbol synchronization [12,25]. In contrast, orthogonal frequency division multiplexing (OFDM) has been widely applied in bandlimited UOWC systems, owing to its high spectral efficiency, simple single-tap equalization, and resistance to inter-symbol interference (ISI), as well as frequency-selective fading [26–28]. Furthermore, it has been shown that the capacity of bandlimited UOWC systems can be further increased by using OFDM with bit and/or power loading [20,29].

Lately, several advanced modulation techniques based on the multi-carrier characteristic of OFDM have been further proposed in the literature, such as OFDM with subcarrier index modulation (OFDM-SIM), OFDM with subcarrier number modulation (OFDM-SNM), OFDM with interleaved subcarrier number modulation (OFDM-ISNM) and so on [30–33].

Photonics **2024**, 11, 1051 3 of 18

Nevertheless, for both OFDM-SIM and OFDM-SNM, the subcarriers in the high-frequency region inevitably suffer from severe power attenuation due to the low-pass frequency response of the bandlimited UOWC system. Although OFDM-ISNM can efficiently enhance the capacity of bandlimited UOWC systems via low-pass-aware signal mapping and subblock interleaving, it might not be feasible for high-spectral-efficiency applications due to the requirement of a relatively large constellation size and the resultant high decoding complexity.

Moreover, it is also a straightforward way to reduce the impact of the low-pass effect by only utilizing a subset of subcarriers for data transmission in the low-frequency region. Nevertheless, for the same transmitted signal power, reducing the number of data subcarriers will lead to an increase in power for each remaining low-frequency data subcarrier. It has been experimentally verified in our previous work [23] that a subcarrier with relatively high power will become much more vulnerable to LED/LD nonlinearity, resulting in much-reduced transmission performance. Also, it has been further experimentally observed in [34] that the high-frequency subcarriers have a larger dynamic range than the low-frequency subcarriers due to the low-pass frequency response. Therefore, for OFDM with a reduced number of data subcarriers, the remaining low-frequency data subcarrier can be extremely vulnerable to LED/LD nonlinearity since the low-frequency dynamic range is relatively small, and the subcarrier power is inevitably increased.

When both the BER and capacity requirements of practical bandlimited UOWC systems are considered, the existing modulation schemes can hardly achieve the flexible trade-off between BER and capacity, and the overall system performance still needs to be substantially enhanced.

## 1.2. Main Contributions

To achieve a BER-capacity trade-off in bandlimited UOWC systems and further enhance the overall system performance, in this paper, we propose a novel orthogonal frequency division diversity and multiplexing (OFDDM) scheme by adopting hybrid diversity and multiplexing transmission among different subcarriers in the frequency domain. The main contributions of this work can be summarized as follows:

- The proposal of a novel OFDDM scheme for bandlimited UOWC systems, which can
  efficiently support a flexible trade-off between BER and capacity so as to adapt to
  various underwater transmission conditions.
- The utilization of subblock interleaving in OFDDM to effectively mitigate the adverse low-pass effect in bandlimited UOWC systems and, hence, extend the effective modulation bandwidth of the system.
- The design of low-complexity, channel-based diversity-combining approaches to reduce the receiver's computational complexity using low-pass channel response estimation, instead of received SNR estimation.
- An evaluation and comparative analysis of the proposed OFDDM scheme against conventional OFDM in various UOWC scenarios via both simulations and experiments, demonstrating the superiority of the proposed scheme.

## 2. System Model

#### 2.1. Principle of OFDDM

Figure 1a,b depict the block diagrams of an OFDDM transmitter and receiver, respectively. For the transmission of each OFDDM block, a total of m input bits enter the OFDDM transmitter. These m bits are first split into G groups, each consisting of b bits, i.e., m = bG, with  $b = \log_2 M$ , where M denotes the order of the adopted quadrature amplitude modulation (QAM) constellation. Each group of b bits is then fed into an OFDDM subblock with length n, with n = N/G and N being the number of data subcarriers. In each subblock, M-QAM mapping is first performed, and all the n subcarriers within the subblock are then employed to simultaneously transmit the resultant M-QAM symbol  $s_g$  through diversity splitting with  $g = 1, \cdots, G$ . As we can see from Figure 1a, the obtained n M-QAM symbols

Photonics **2024**, 11, 1051 4 of 18

after diversity splitting are denoted as  $s_g^{(1)}, \dots, s_g^{(n)}$ , and we have  $s_g^{(1)} = \dots = s_g^{(n)} = s_g$ . Hence, the subcarriers within each subblock transmit the same M-QAM symbol via diversity transmission, while different subblocks transmit different M-QAM symbols via multiplexing transmission. As a result, hybrid diversity and multiplexing transmission can be supported in the proposed OFDDM scheme. For each subblock in OFDDM, the subblock spectral efficiency (bit/s/Hz) is given by

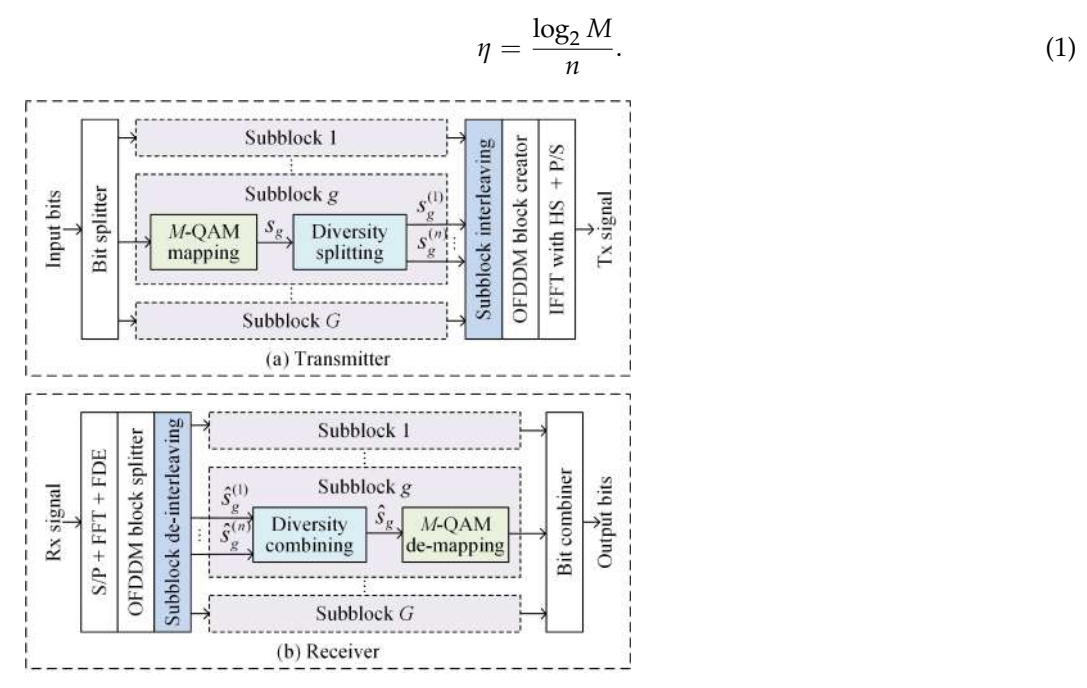


Figure 1. Block diagram of OFDDM: (a) transmitter and (b) receiver.

Subsequently, subblock interleaving is executed to mitigate the adverse low-pass effect of the bandlimited UOWC system, and the detailed principle of subblock interleaving will be introduced in the next subsection. After the concatenation of *G* subblocks, the whole OFDDM block is created. Finally, the transmitted OFDDM signal is obtained by performing an inverse fast Fourier transform (IFFT) with Hermitian symmetry (HS) and parallel-to-serial (P/S) conversion [28].

In the OFDDM receiver, as shown in Figure 1b, the received OFDDM signal undergoes serial-to-parallel (S/P) conversion, FFT, and frequency-domain equalization (FDE). The resultant OFDDM block is split into G subblocks, and subblock de-interleaving is further executed. After that, diversity combining is carried out to obtain the estimate of the transmitted M-QAM symbol  $\hat{s}_g$  from the received n M-QAM symbols  $\hat{s}_g^{(1)}, \cdots, \hat{s}_g^{(n)}$  with respect to the n subcarriers in the subblock. In order to reduce the computational complexity of diversity combining, low-complexity diversity-combining approaches are proposed, and the detailed principle will be discussed later. Finally, the transmitted bits of each subblock can be recovered via M-QAM demapping, and the output bits of the whole OFDDM block can be generated by combining the recovered bits of each subblock together.

To better describe the principle of the proposed OFDDM scheme, we define the diversity factor, d, as the number of subcarriers that transmit the same symbol in one subblock. Under the assumption that all the n subcarriers in each subblock are utilized to transmit the same symbol, we have d=n. Figure 2 illustrates the OFDDM spectrum with different diversity factors, where a total of N=8 data subcarriers are considered. For the case of d=1, as shown in Figure 2a, the number of transmitted symbols is exactly the same as the number of data subcarriers, i.e.,  $N_{\rm symbol}=N=8$ , and hence, OFDDM with d=1 is equivalent to conventional OFDM. For the case of d=2, as can be seen from Figure 2b, the subcarriers are uniformly partitioned into four subblocks, and the two subcarriers within each subblock transmit the same symbol. Figure 2c shows the case for d=4 and the same symbol is

Photonics **2024**, 11, 1051 5 of 18

transmitted via the four subcarriers within each subblock. For the case of d=8, as shown in Figure 2d, all eight subcarriers are used to transmit the same symbol, and this scheme can be called orthogonal frequency division diversity (OFDD). It can be clearly observed from Figure 2 that OFDM and OFDD are two extreme cases of the proposed OFDDM scheme. Moreover, for a fixed M-QAM constellation, we can achieve a flexible trade-off between diversity and multiplexing in OFDDM by adjusting the diversity factor, d.

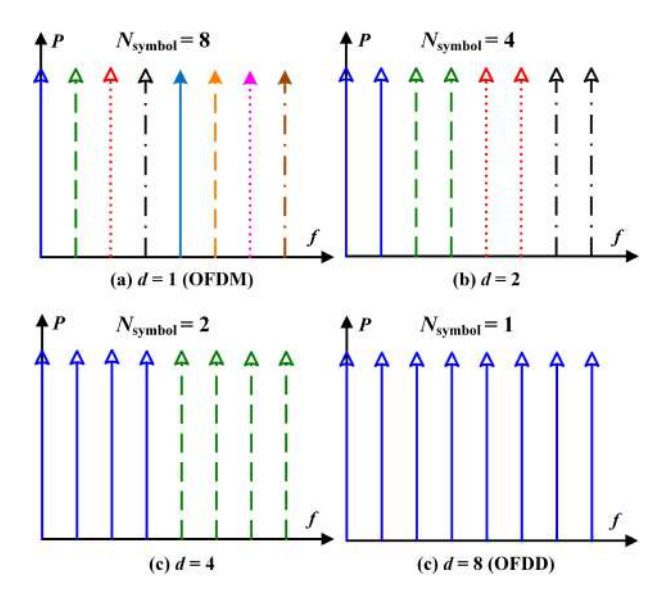


**Figure 2.** Illustration of OFDDM spectrum with different diversity factors: (a) d = 1, (b) d = 2, (c) d = 4, and (d) d = 8.

Although it is also feasible to use only N/d subcarriers at the low-frequency region in OFDM to overcome the low-pass effect, the reduction in the subcarrier number will inevitably lead to an increase in the subcarrier power for a given transmitted signal power, which will make the OFDM signal vulnerable to the limited dynamic range and nonlinearity of the light source in practical UOWC systems [23,34]. In contrast, OFDDM has the same number of subcarriers for signal transmission as in OFDM, and therefore, OFDDM can be effectively implemented based on the existing OFDM system without adjusting the number of subcarriers for signal transmission. In conclusion, the motivation to use the proposed OFDDM scheme instead of OFDM with a reduced bandwidth/number of data subcarriers is mainly due to its following two advantages: (1) enhanced robustness against LED/LD nonlinearity and (2) total compatibility with standard OFDM transceiver hardware implementation.

# 2.2. Subblock Interleaving

In order to address the low-pass frequency response effect of the bandlimited UOWC system, subblock interleaving is performed at the transmitter side. Figure 3a,b illustrate the transmitted OFDDM spectrum without and with subblock interleaving, respectively, by taking N=8 and d=2 as an example. For the case without subblock interleaving, as shown in Figure 3a, the subcarriers in each subblock are sequentially distributed within the corresponding region of the subblock. In contrast, for the case with subblock interleaving, as shown in Figure 3b, the subcarriers in each subblock are not adjacent to each other but distributed cross the entire frequency band. After passing through the low-pass UOWC channel, the received OFDDM spectrum without and with subblock interleaving is shown in Figure 3c,d, respectively. It can be clearly observed from Figure 3c that the subblocks in the high-frequency region suffer from much more severe power attenuation than those in the low-frequency region. Nevertheless, when adopting subblock interleaving, as shown in Figure 3d, the subcarriers within each subblock are staggered and separated in the frequency band. Consequently, the unfairness of attenuation between subblocks can be

Photonics **2024**, 11, 1051 6 of 18

efficiently mitigated by employing subblock interleaving. Nevertheless, subblock unfairness still exists due to the adopted sequential subblock interleaving approach and more advanced subblock interleaving approaches that can further enhance subblock fairness will be considered in our future work.

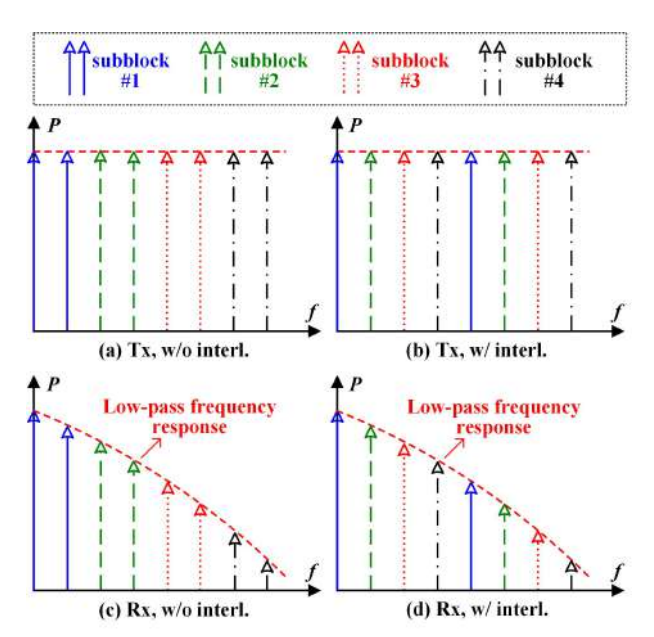


**Figure 3.** Illustration of OFDDM spectrum: (a) Tx, without interleaving, (b) Tx, with interleaving, (c) Rx, without interleaving, and (d) Rx, with interleaving; w/o: without, w/: with, interl.: interleaving.

## 2.3. Low-Complexity Channel-Based Diversity Combining

To reduce the computational complexity of diversity combining at the receiver side in OFDDM, we further propose low-complexity channel-based diversity-combining approaches using the estimated low-pass channel frequency response information, instead of the estimated received SNR information.

Let  $y_{g,l}$  denote the received M-QAM symbol on the l-th subcarrier in g-th subblock with  $l=1,\cdots,n$  and  $g=1,\cdots,G$ , which can be expressed as

$$y_{g,l} = h_0 h(f_{g,l}) x_g + n_{g,l}, (2)$$

where  $x_g$  is the M-QAM symbol transmitted via all the n subcarriers in the g-th subblock,  $h_0$  is the overall channel gain due to channel transmission, which is a constant value for all the subcarriers,  $h(f_{g,l})$  is the channel gain of the l-th subcarrier in the g-th subblock resulting from the low-pass frequency response of the system, which is a function of the subcarrier frequency,  $f_{g,l}$ , and  $n_{g,l}$  is the corresponding additive white Gaussian noise (AWGN). After performing FDE, the equalized signal on the l-th subcarrier in the g-th subblock can be represented as

$$\hat{x}_{g,l} = x_g + \frac{n_{g,l}}{h_0 h(f_{g,l})}. (3)$$

With  $P_s^f$  and  $P_n^f$  denote the transmitted signal power and the noise power of each subcarrier in the frequency domain, respectively, the received SNR of the l-th subcarrier in the g-th subblock is given by

$$\gamma_{g,l} = \frac{h_0^2 P_s^f}{P_n^f} h^2(f_{g,l}) = \gamma_0^f h^2(f_{g,l}) \propto h^2(f_{g,l}). \tag{4}$$

where  $\gamma_0^f = h_0^2 P_s^f / P_n^f$  is the received SNR without the impact of the low-pass effect. Since  $h_0$ ,  $P_s^f$  and  $P_n^f$  are all constant values for all the subcarriers, the received SNR,  $\gamma_0^f$ , is a

Photonics **2024**, 11, 1051 7 of 18

constant value, and hence, the received SNR of the l-th subcarrier in the g-th subblock is linearly proportional to the square of  $h(f_{g,l})$ , i.e.,  $h^2(f_{g,l})$ .

The above observation motivates us to utilize the estimated low-pass channel frequency response information, i.e.,  $h(f_{g,l})$ , to efficiently perform diversity combining with low computational complexity at the receiver side. Specifically, equal-gain combining (EGC) is the simplest diversity-combining approach that directly combines all the signals obtained within the same subblock, together with the same weight, i.e,  $\hat{x}_{g,EGC} = \frac{1}{d} \sum_{l=1}^{d} \hat{x}_{g,l}$  [35]. Hence, the resultant SNR of the combined signal using EGC can be given by

$$\gamma_{g,EGC} = \left(\frac{\sum_{l=1}^{d} h(f_{g,l})}{n}\right)^{2} \gamma_{0}^{f}. \tag{5}$$

Considering that the EGC approach is not dependent on the channel frequency response or the received SNR, we mainly introduce two channel-based diversity-combining approaches, including select-best combining (SC) and maximal-ratio combining (MRC), in the following [36].

## 2.3.1. Channel-Based SC

In the channel-based SC, the index of the subcarrier that has the largest channel frequency response in the *g*-th subblock is first identified:

$$l_g = \underset{l}{\operatorname{argmax}} \{ h^2(f_{g,l}) \}, \tag{6}$$

and then the combined signal of the g-th subblock using channel-based SC can be expressed by,

$$\hat{x}_{g,SC} = \hat{x}_{g,l_g},\tag{7}$$

and the resultant SNR of the combined signal using channel-based SC can be given by

$$\gamma_{g,SC} = h^2(f_{g,l_g})\gamma_0^f. \tag{8}$$

#### 2.3.2. Channel-Based MRC

In the channel-based MRC, the combined signal of the g-th subblock is obtained using the estimated low-pass channel frequency response information, i.e.,  $h(f_{g,l})$ , as follows:

$$\hat{x}_{g,MRC} = \alpha \sum_{l=1}^{d} h^2(f_{g,l}) \hat{x}_{g,l},$$
(9)

where  $\alpha = 1/\sum_{l=1}^{d} h^2(f_{g,l})$  denotes the power normalization factor. Accordingly, the resultant SNR of the combined signal using channel-based MRC can be given by [37]

$$\gamma_{g,MRC} = \sum_{l=1}^{d} \gamma_{g,l} = \sum_{l=1}^{d} h^2(f_{g,l}) \gamma_0^f.$$
 (10)

Based on the obtained SNRs, the corresponding theoretical BERs can be calculated using the BER expression given by Eq. (9) in [37].

#### 3. Results and Discussions

In this section, both simulations and experiments are conducted to evaluate and compare the performance of the proposed OFDDM scheme with the conventional OFDM scheme.

Photonics **2024**, 11, 1051 8 of 18

## 3.1. Simulation Results

In the simulations, a bandlimited UOWC system over an AWGN channel with a low-pass frequency response measured from the experimental UOWC system is considered, where the overall channel gain,  $h_0$ , is assumed to be 1, and the time-domain SNR is defined by  $\gamma^t = P_s^t/P_n^t$ , with  $P_s^t$  and  $P_n^t$  denoting the transmitted signal power and the noise power of each subcarrier in the time domain, respectively. Figure 4 depicts the measured electrical–electrical (EOE) low-pass frequency response, where the -3 dB modulation bandwidth is 620 MHz. The adopted EOE low-pass frequency response is measured from our established experimental system, which can be found in detail in Section 3.2. Additionally, the length of IFFT,  $N_{\rm ifft}$ , and the number of data subcarriers,  $N_s$ , in OFDDM modulation is set to 256 and 108, respectively.

Figure 5 shows the achievable spectral efficiency versus constellation order M for OFDDM with different diversity factors. It is worth mentioning that subblock interleaving has no effect on the achievable spectral efficiency of OFDDM. As can be seen in Figure 5, greater spectral efficiency is obtained with a smaller diversity factor, d, for a given constellation order, M. Moreover, to achieve the same spectral efficiency, a smaller M can be used when a smaller d is adopted. In the following, four different spectral efficiencies, i.e., 1, 1.5, 2, and 2.5 bits/s/Hz, are considered for performance evaluation, and the required constellation orders, M, can be obtained from Figure 5 so as to ensure the same target spectral efficiency for all the considered schemes.

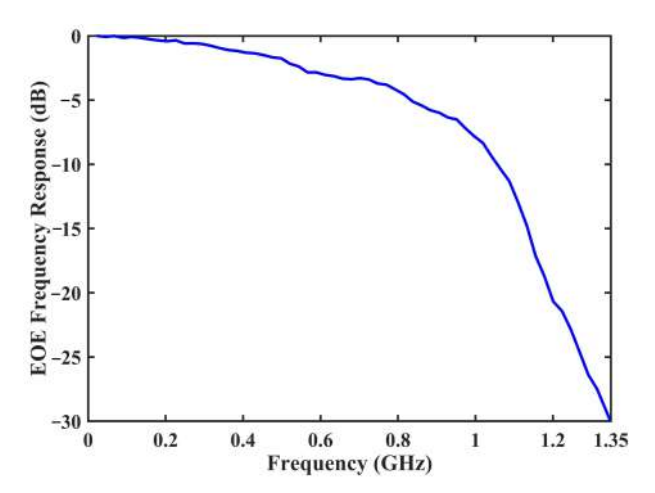
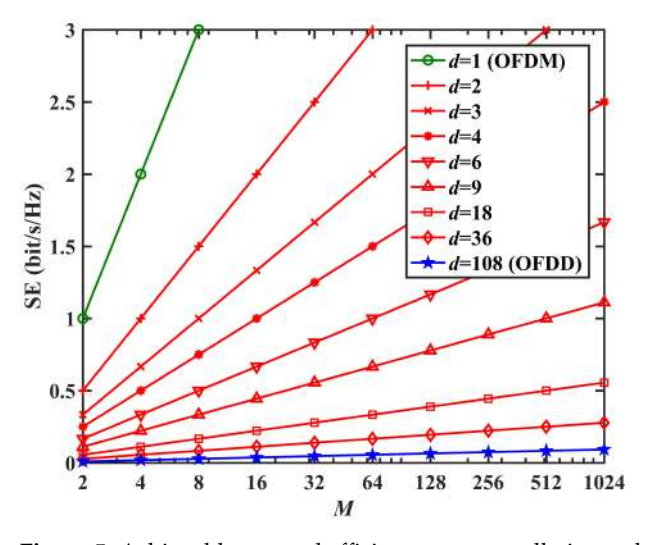


Figure 4. Measured frequency response from the experimental UOWC system.



**Figure 5.** Achievable spectral efficiency vs. constellation order *M* for OFDDM with different diversity factors.

Photonics **2024**, 11, 1051 9 of 18

Figure 6a-c show the simulation BER performance versus SNR for OFDDM using channel-based diversity, combining with M=4 and d=2,4 over the AWGN channel, the low-pass channel without interleaving, and the low-pass channel with interleaving, respectively. For the AWGN channel, MRC and EGC obtain the same BER performance with the same diversity factor, d, while SC with d = 2 performs the same as SC with d = 4. For the low-pass channel without interleaving, MRC and EGC also achieve comparable BER performance with the same diversity factor, *d*, which is mainly due to the negligible low-pass effect within each subblock. In contrast, SC with d=4 outperforms SC with d=2since the channel gain/SNR of the selected subcarrier is relatively larger when performing SC with a larger d. For the low-pass channel with interleaving, MRC and SC with d = 2 have comparable BER performance, which is because the two subcarriers within each subblock have very distinctive channel gains/SNRs. Moreover, MRC with d = 4 performs the best, and SC with d=4 also outperforms MRC or SC with d=2, while EGC, with either d=2or d = 4, it performs at least 15 dB worse than MRC or SC with d = 2 at the 7% forward error correction (FEC) coding threshold of BER =  $3.8 \times 10^{-3}$ . This is because EGC simply combines the branches within each subblock with equal weights. Due to the pronounced differences in channel gains across branches, the addition of branches with lower channel gains introduces more noise power relative to the signal power, consequently leading to degraded performance. It can be concluded from Figure 6 that MRC always achieves the best performance, as expected, and hence, it is used in the following performance evaluations. Figure 7a,b show the theoretical and simulation BER performance versus SNR for OFDDM using channel-based diversity combining with M = 4 and d = 2,4 over the low-pass channel without and with interleaving, respectively. As we can clearly observe, the simulation results agree well with the theoretical results.

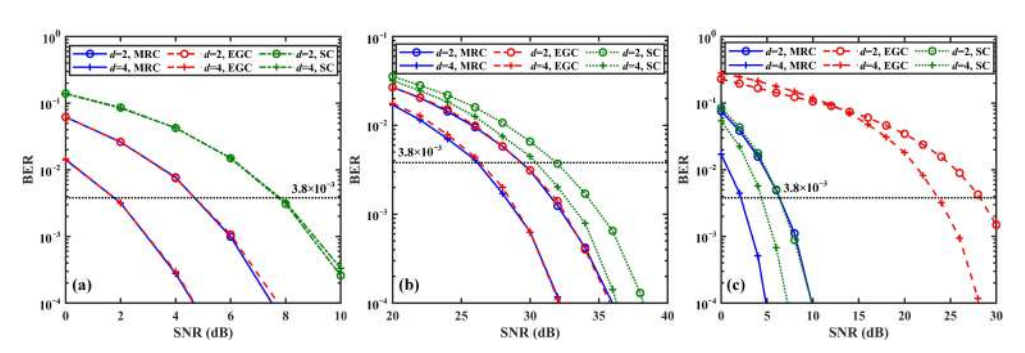


**Figure 6.** Simulation BER vs. SNR for OFDDM using channel-based diversity combining with M=4 and d=2,4 over (a) the AWGN channel, (b) the low-pass channel without interleaving, and (c) the low-pass channel with interleaving.

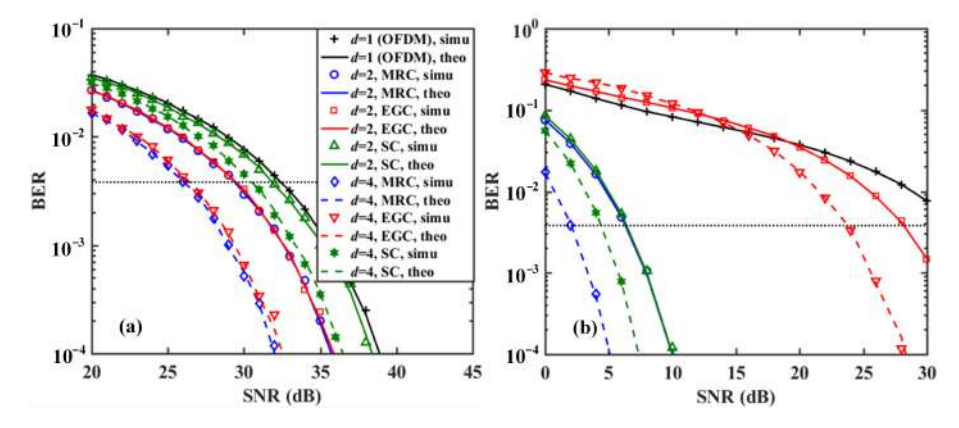


**Figure 7.** Theoretical and simulation BER vs. SNR for OFDDM using channel-based diversity, combining with M=4 and d=2,4: (a) the low-pass channel without interleaving and (b) the low-pass channel with interleaving.

Photonics **2024**, 11, 1051 10 of 18

Figure 8 shows the simulation BER performance versus SNR for OFDDM with M=2 and different diversity factors over different channels without and with interleaving. For the AWGN channel, as shown in Figure 8a, a better BER performance is obtained when a larger diversity factor, d, is considered. More specifically, a 3 dB SNR gain can be obtained when the diversity factor d is increased from 1 to 2, which is because the use of MRC can double the SNR over the AWGN channel. Figure 8b,c present the BER performance versus SNR over the low-pass channel without and with interleaving, respectively. Similarly, the use of a larger diversity factor, d, inevitably results in better BER performance. However, for the case without interleaving, the SNR gain is also only about 3 dB when d is increased from 1 to 2. In contrast, for the case with interleaving, a significant SNR gain of 26.1 dB can be achieved at the 7% FEC coding threshold of BER =  $3.8 \times 10^{-3}$  when d is increased from 1 to 2.

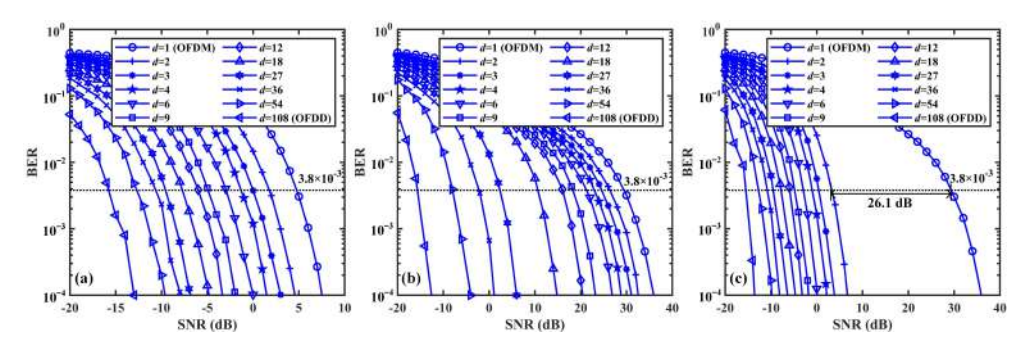


**Figure 8.** Simulation BER vs. SNR for OFDDM with M=2 and different diversity factors over (a) the AWGN channel, (b) the low-pass channel without interleaving, and (c) the low-pass channel with interleaving.

According to (1), it is known that the subblock spectral efficiency of OFDDM is gradually reduced with the increase in the subblock length, n. In order to better reflect the impact of diversity transmission on the subblock spectral efficiency of OFDDM for an arbitrary constellation order, M, we define the normalized spectral efficiency  $\eta_{\text{norm}}$  as follows:

$$\eta_{\text{norm}} = \frac{\eta}{\log_2 M} = \frac{1}{n}.\tag{11}$$

Using n=d under the assumption that all the n subcarriers in each subblock are utilized to transmit the same symbol, we have  $\eta_{\text{norm}}=1/d$ . Moreover, we further define the SNR margin  $\delta_{\text{SNR}}$  as the difference between the SNR required for conventional OFDM and that for the proposed OFDDM to reach a certain BER threshold, e.g., 7% FEC coding threshold of BER =  $3.8 \times 10^{-3}$ , for a given M-QAM constellation. Since conventional OFDM can be considered OFDDM with d=1, the transmitted power of the constellation symbol is enlarged by d times in comparison to conventional OFDM for MRC-based OFDDM with an arbitrary diversity factor, d. As a result, the required SNR to reach the BER threshold of  $3.8 \times 10^{-3}$  is reduced by d times, and accordingly, the SNR margin  $\delta_{\text{SNR}}$  in decibels can be obtained by

$$\delta_{\text{SNR}} = 10 \log_{10} d. \tag{12}$$

Since  $\eta_{\text{norm}} = 1/d$ , we can obtain the relationship between the SNR margin,  $\delta_{\text{SNR}}$ , and the normalized spectral efficiency,  $\eta_{\text{norm}}$ , as follows

$$\delta_{\rm SNR} = 10 \log_{10} \left( \frac{1}{\eta_{\rm norm}} \right). \tag{13}$$

Figure 9 depicts the available SNR margin versus normalized spectral efficiency for OFDDM in comparison to conventional OFDM, where the theoretical results are obtained using (13), while the simulation results are obtained from Figure 8a. As we can see, the available SNR margin gradually decreases with the increase in the normalized spectral efficiency. Since a larger SNR margin indicates a lower BER that the system can have,

while a larger normalized spectral efficiency suggests a higher capacity that the system can achieve, it is feasible to realize the flexible trade-off between BER and capacity by adjusting the diversity factor, *d*. Moreover, it is also found that the simulation results achieve a very good match with the theoretical curve.

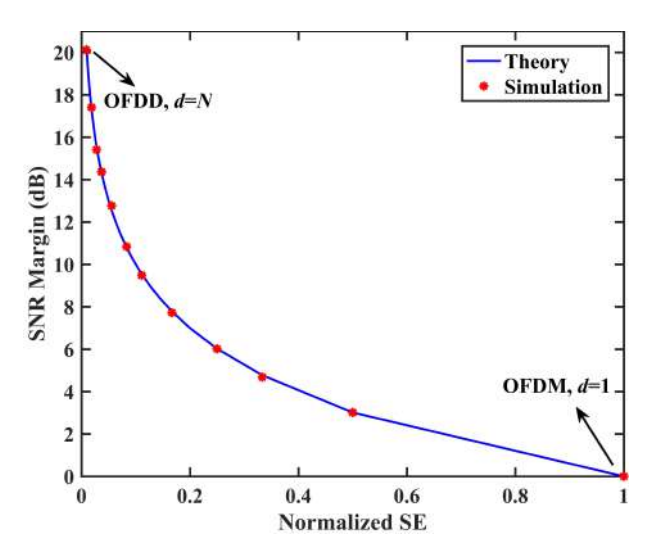


**Figure 9.** Available SNR margin vs. normalized spectral efficiency for OFDDM in comparison to conventional OFDM.

In order to show the ability to use OFDDM to achieve a flexible trade-off between BER and capacity in UOWC systems, we further investigate the BER performance of the UOWC system using OFDDM over an AWGN channel with an SNR of 15 dB and M=2, where the line-of-sight (LOS) channel gain is calculated by using the model and parameters in [38]. Figure 10 depicts the simulation BER versus the transmission distance using OFDDM over a low-pass channel, where OFDDM with different d values is considered. As we can see, within the distance range from 0 to 0.92 m, OFDDM with d = 1, i.e., conventional OFDM, can achieve a BER under the 7% FEC coding threshold of  $3.8 \times 10^{-3}$ . However, for a distance larger than 0.92 m, it is impossible for conventional OFDM to reach the BER threshold. As a result, OFDDM with a larger diversity factor, e.g., d = 2, can be used to reduce the BER by sacrificing the capacity of the system. Specifically, OFDDM with d=2can guarantee an effective transmission distance of up to 3.7 m, while a relatively large diversity factor of d = 5 is required to reach the transmission distance of 5 m. It can be observed from Figure 10 that OFDDM is indeed able to make the trade-off between BER and capacity by selecting a proper diversity factor, *d*, according to the specific channel conditions.

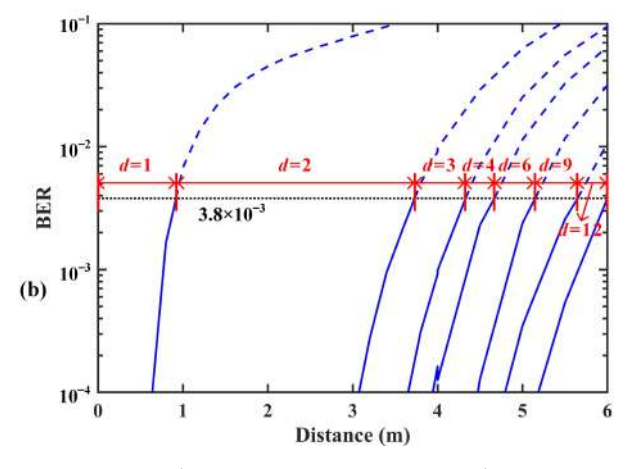
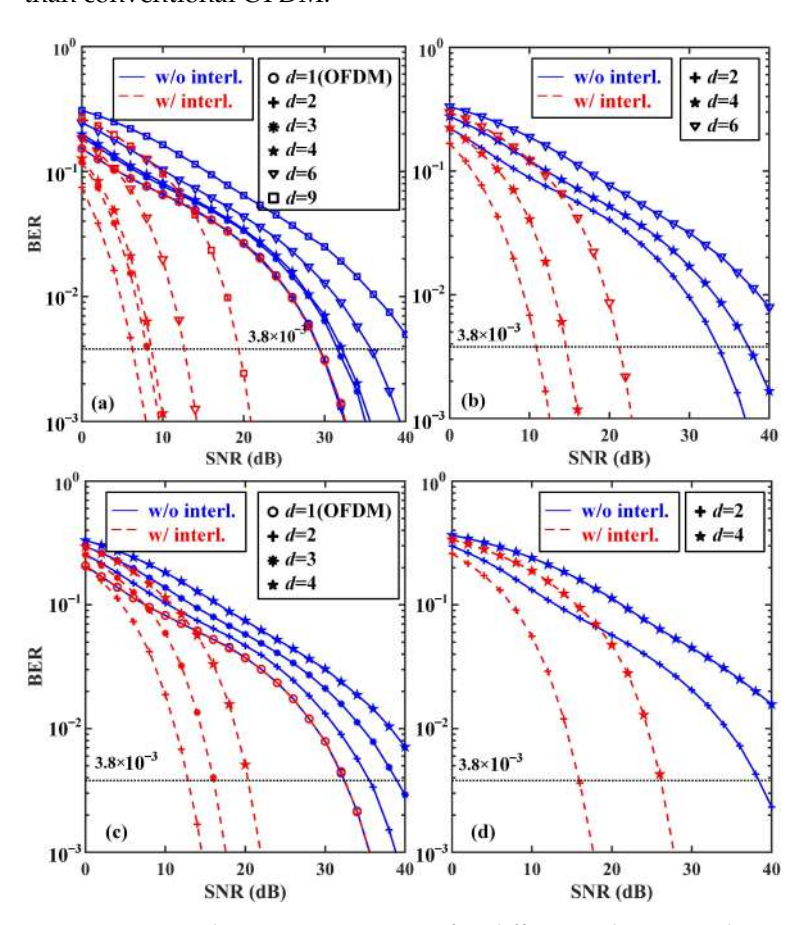


Figure 10. Simulation BER vs. transmission distance using OFDDM over a low-pass channel.

In addition to the flexible trade-off between BER and capacity, we also evaluate and compare the BER performance of OFDDM schemes with different d values to achieve the same target spectral efficiency over the low-pass channel without and with interleaving. To reach a target spectral efficiency, the required constellation order, M, can be obtained from Figure 5. Figure 11 presents the simulation BER versus SNR for different schemes with the same target spectral efficiency. For a target spectral efficiency of 1 bit/s/Hz, as depicted in Figure 11a, an SNR of 29.4 dB is needed for conventional OFDM to reach  $BER = 3.8 \times 10^{-3}$ , while OFDDM with interleaving can greatly outperform conventional OFDM when a proper diversity factor, d, is selected. As can be seen, interleaved OFDDM with d = 2 only requires an SNR of as low as 6.2 dB to reach the BER threshold, which indicates a very significant SNR gain of 23.2 dB in comparison to conventional OFDM. When the target spectral efficiency is increased to 1.5, 2, and 2.5 bits/s/Hz, as is respectively shown in Figure 11b-d, the best BER performance is always obtained by interleaved OFDDM with d=2. It can be generally concluded from Figure 11 that subblock interleaving is necessary for OFDDM to overcome the adverse low-pass effect, and the selection of an optimal diversity factor, d, plays a vital role for OFDDM to achieve superior performance than conventional OFDM.



**Figure 11.** Simulation BER vs. SNR for different schemes with a target spectral efficiency of (a) 1 bit/s/Hz, (b) 1.5 bits/s/Hz, (c) 2 bits/s/Hz, and (d) 2.5 bits/s/Hz.

# 3.2. Experimental Results

We further conduct hardware experiments to investigate and compare the performance of the proposed OFDDM scheme with conventional OFDM in practical UOWC systems. The experimental setup of the UOWC system that utilizes a vertical-cavity-emitting laser (VCSEL) as an optical transmitter is depicted in Figure 12. As we can see, the transmitted signal is first generated offline via MATLAB and then uploaded to an arbitrary waveform generator (AWG, Tektronix AWG7101) with a 10-bit vertical resolution and a maximum sampling rate of 10 GSa/s. Subsequently, a DC bias current is combined with the AWG

output signal via a bias-tee (bias-T, Mini-circuit ZFBT-6GW+), and the resultant signal is employed to drive the VCSEL (DERAY DV0688M). The light emitted via the VCSEL passes through a biconvex lens and propagates through a 2 m water tank. At the receiver side, another biconvex lens is used to focus the light onto the active area of an avalanche photodiode (APD, Menlo Systems APD210) with a -3 dB bandwidth of about 1 GHz and a frequency range from 1 MHz to 1.6 GHz. After that, the output electrical signal of the APD is recorded via a digital storage oscilloscope (DSO, Tektronix MSO73304DX) with an 8-bit vertical resolution and a fixed sampling rate of 25 GSa/s, and the resultant digital signal is further processed offline via MATLAB. Moreover, the corresponding parameters of OFDDM modulation are the same as that in simulations. To better describe the obtained experimental results, we here define the effective bandwidth as  $B_{\rm eff} = NR_{\rm s}/N_{\rm ifft}$ , where  $R_{\rm s}$  denotes the AWG sampling rate.

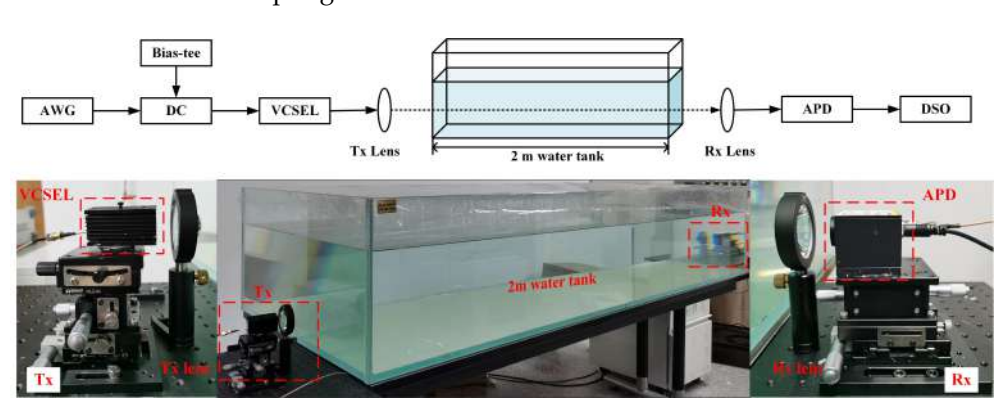


Figure 12. Experimental setup of the VCSEL-based UOWC system.

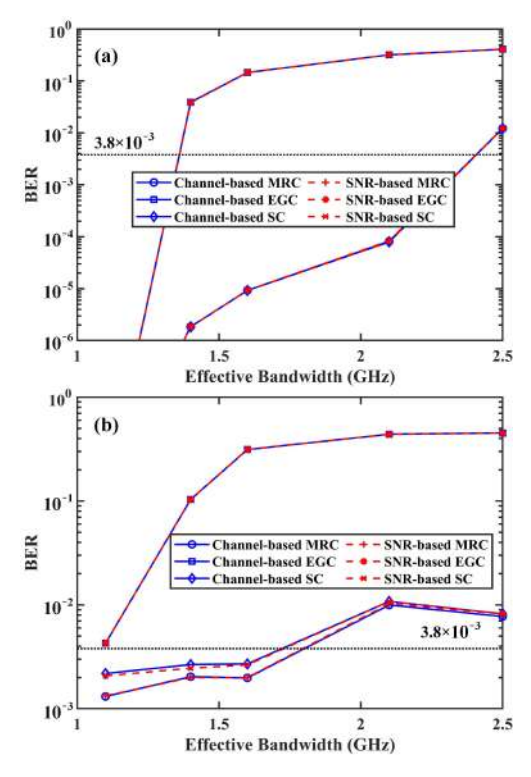
Figure 13a,b show the experimental BER performance versus effective bandwidth for OFDDM using both SNR-based and channel-based diversity-combining approaches with d=2 and 4, respectively. It can clearly be observed that the proposed low-complexity channel-based diversity-combining approaches achieve exactly the same BER performance as the conventional SNR-based diversity-combining approaches for both d=2 and 4. Moreover, MRC and SC perform comparably for d=2, while MRC outperforms SC for d=4, which agrees well with the results shown in Figure 6c. Due to its low complexity and excellent performance, channel-based MRC is adopted to perform diversity combining in OFDDM in the following experimental investigations.

Figure 14 shows the experimental BER performance versus diversity factor d for OFDDM without and with interleaving at different effective bandwidths, where the target spectral efficiency is 1 bit/s/Hz. For the case without interleaving, OFDDM with d=1, i.e., conventional OFDM, always obtains the lowest BER for all the considered effective bandwidths. In contrast, for the case with interleaving, the BERs at different effective bandwidths first decrease and then increase with the increase in the diversity factor, d, and there exists an optimal d to yield the minimum BER at each effective bandwidth. More specifically, the optimal d value for relatively small effective bandwidths of 1.1, 1.4, 1.6, and 2.1 GHz is 2, while it is increased to 3 for relatively large effective bandwidths of 2.5 and 3.0 GHz. This indicates that a larger diversity gain is needed to overcome the much more severe low-pass effect when the effective bandwidth becomes larger.

Figure 15 depicts the experimental BER versus effective bandwidth for conventional OFDM and OFDDM with optimal d at a target spectral efficiency of 1 bit/s/Hz. As we can see, the maximum achievable effective bandwidths with respect to the 7% FEC coding threshold of BER =  $3.8 \times 10^{-3}$  are 1.32 and 2.72 GHz for conventional OFDM and OFDDM with optimal d, respectively. Therefore, a striking effective bandwidth extension of 106.1% can be achieved using OFDDM with an optimal d in comparison to conventional OFDM. Since the same target spectral efficiency of 1 bit/s/Hz is considered for both schemes, OFDDM with an optimal d obtains a more than doubled capacity compared to conventional OFDM.

Photonics **2024**, 11, 1051 14 of 18

In addition to fixed bit loading to achieve a given target spectral efficiency, we further consider adaptive bit loading in OFDDM. Figure 16 depicts the bit loading profile versus subcarrier/subblock for OFDM/OFDDM with d=2 and interleaving, where the total 108 data subcarriers in OFDM are divided into 54 subblocks when performing OFDDM with d=2. For conventional OFDM, i.e., OFDDM with d=1, the maximum number of bits that can be loaded via subcarriers is 5, which is mainly obtained using the first 20 subcarriers in the low-frequency region. Moreover, only the first 50 subcarriers among a total of 108 data subcarriers can be used to carry data, while the remaining subcarriers are left unloaded due to their sufficiently low SNRs. In contrast, for OFDDM with d=2, 50 out of 54 subblocks can be utilized to carry data, and the maximum number of bits that can be loaded reaches 6, which is mainly due to the substantial SNR enhancement resulting from the diversity transmission within each subblock. The insets in Figure 16 depict the corresponding received constellation diagrams for OFDDM with d=2.



**Figure 13.** Experimental BER vs. effective bandwidth for OFDDM using SNR-based and channel-based diversity-combining approaches with (a) d = 2 and (b) d = 4.

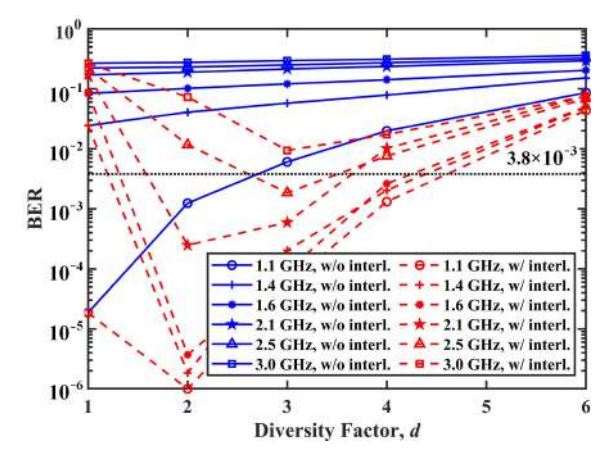


**Figure 14.** Experimental BER vs. diversity factor *d* for OFDDM without and with interleaving at different effective bandwidths at a target spectral efficiency of 1 bit/s/Hz.

Photonics **2024**, 11, 1051 15 of 18

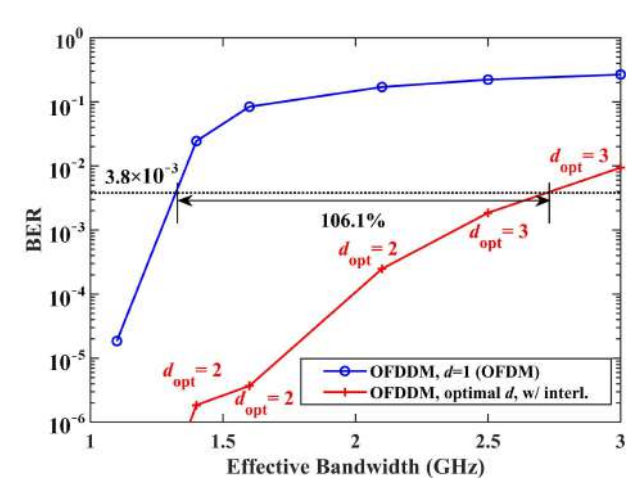


**Figure 15.** Experimental BER vs. effective bandwidth for conventional OFDM and OFDDM with optimal d at a target spectral efficiency of 1 bit/s/Hz.

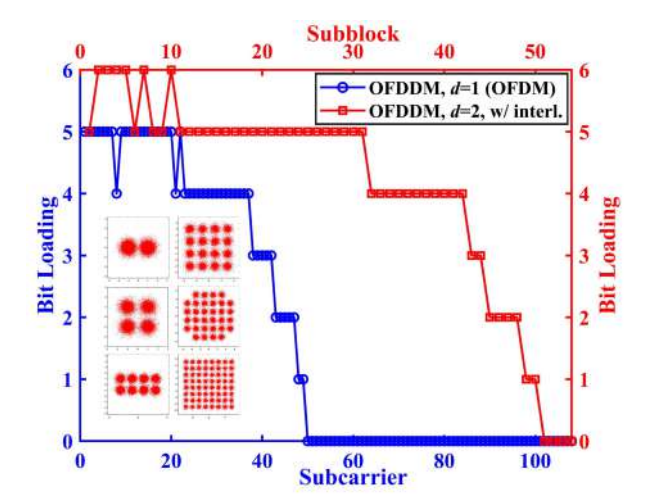
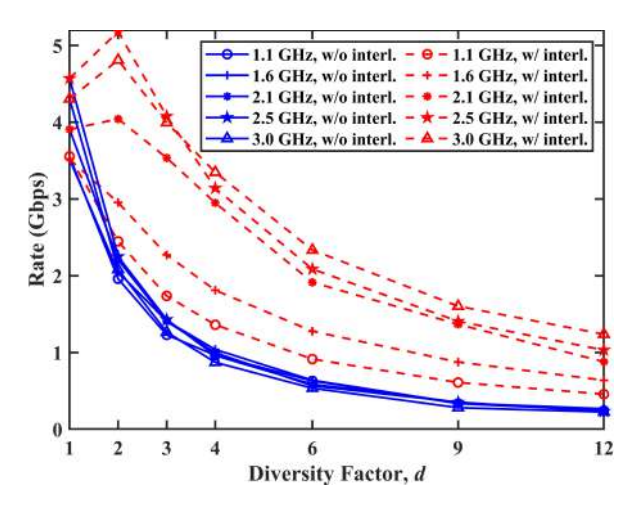


**Figure 16.** Bit loading vs. subcarrier/subblock for OFDM/OFDDM with d=2. Insets show the corresponding received constellation diagrams for OFDDM with d=2.

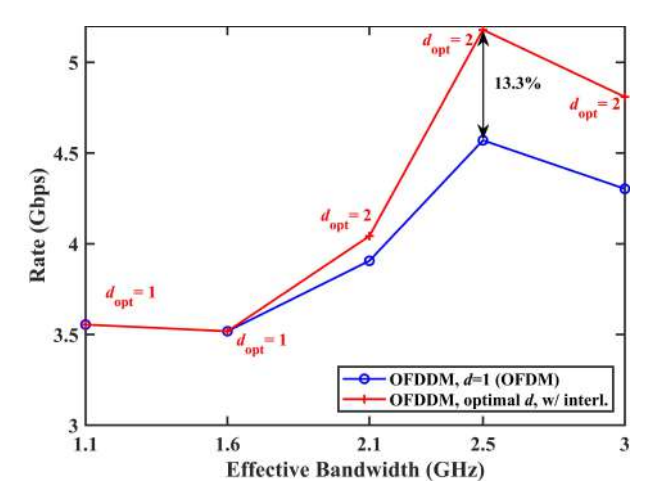
Figure 17 shows the achievable rate versus diversity factor d for OFDDM with adaptive bit loading at different effective bandwidths. It can be clearly observed that the maximum achievable rate without interleaving is always obtained using OFDDM with d=1, i.e., conventional OFDM. However, for OFDDM with interleaving, we can see that there exists an optimal d value of 2 for OFDDM to achieve the maximum achievable rate at relatively large effective bandwidths of 2.1, 2.5, and 3.0 GHz. As a result, OFDDM with adaptive bit loading is capable of outperforming conventional OFDM with adaptive bit loading in terms of the achievable rate when the effective bandwidth is relatively large and the low-pass effect is relatively severe.

Figure 18 shows the achievable rate versus the effective bandwidth for conventional OFDM and OFDDM with optimal d values. As we can see, there exists an optimal effective bandwidth of 2.5 GHz to maximize the achievable rate for both conventional OFDM and OFDDM with optimal d values. At the optimal effective bandwidth of 2.5 GHz, the maximum achievable rates for conventional OFDM and OFDDM with optimal d values are 4.57 and 5.18 Gbps, respectively. Therefore, a remarkable 13.3% capacity improvement can be achieved via OFDDM with optimal d values in comparison to conventional OFDM under the adaptive bit-loading scenarios.

Photonics **2024**, 11, 1051 16 of 18



**Figure 17.** Achievable rate vs. diversity factor *d* for OFDDM with adaptive bit loading at different effective bandwidths.



**Figure 18.** Achievable rate vs. effective bandwidth for conventional OFDM with adaptive bit loading and OFDDM with adaptive bit loading with optimal *d*.

#### 4. Conclusions

In this paper, we have proposed and investigated a novel OFDDM scheme for practical bandlimited UOWC systems. Compared with conventional OFDM, which employs all the data subcarriers to transmit different constellation symbols via a pure multiplexing transmission, the proposed OFDDM scheme adopts a hybrid diversity and multiplexing transmission manner by grouping subcarriers into a subblock to transmit the same constellation symbol. Hence, adaptive diversity and multiplexing transmission can be achieved by dynamically selecting a proper diversity factor when implementing OFDDM. Considering the low-pass effect of the UOWC system and the complexity issue associated with conventional SNR-based diversity combining, subblock interleaving and low-complexity diversity combining have been further proposed. Simulation and experimental results have demonstrated that the proposed OFDDM scheme can achieve a flexible trade-off between BER and capacity so as to adapt to various channel conditions, which can also greatly outperform conventional OFDM achieving the same target spectral efficiency or adopting adaptive bit loading. Therefore, the proposed OFDDM scheme can be a promising candidate for reliable and high-speed 6G UOWC systems.

Although this current work has focused on point-to-point OFDDM transmission in UOWC systems, it is also feasible to enable multiple access using the proposed OFDDM scheme. In orthogonal frequency-division multiple access (OFDMA), multiple access is achieved via subcarrier allocation among different users [39]. Moreover, we have previously proposed an orthogonal subblock-division multiple-access (OSDMA) scheme for

Photonics 2024, 11, 1051 17 of 18

index modulation-aided OFDM systems via subblock allocation in [40]. In our future work, we will investigate OFDDM-based multiple-access schemes via subblock allocation for multi-user OWC systems in which the subblock diversity factor for each user will be adaptively optimized. In addition, the mitigation of turbulence-induced fading in UOWC systems will be further investigated by performing hybrid time/frequency-domain diversity transmission using OFDDM.

**Author Contributions:** Formal analysis, J.C., C.C., and Z.Z.; funding acquisition, C.C.; investigation, J.C. and Z.Z.; methodology, J.Y. and C.H.; project administration, C.C. and M.L.; resources, S.H. and H.Y.F.; software, J.Y.; supervision, C.C., M.L., and H.H.; validation, J.C.; writing—original draft, J.C.; writing—review and editing, C.C., M.L., H.Y.F., and H.H. All authors have read and agreed to the published version of the manuscript.

**Funding:** This research was funded by the National Natural Science Foundation of China (62271091) and the Natural Science Foundation of Chongqing (cstc2021jcyj-msxmX0480).

**Institutional Review Board Statement:** Not applicable.

**Informed Consent Statement:** Not applicable.

Data Availability Statement: Data are contained within the article.

**Acknowledgments:** The authors would like to thank the anonymous reviewers for their valuable comments and suggestions.

**Conflicts of Interest:** The authors declare no conflict of interest.

#### References

1. Wang, C.X.; You, X.; Gao, X.; Zhu, X.; Li, Z.; Zhang, C.; Wang, H.; Huang, Y.; Chen, Y.; Haas, H.; et al. On the road to 6G: Visions, requirements, key technologies, and testbeds. *IEEE Commun. Surv. Tutor.* **2023**, 25, 905–974.

- 2. Singh, P.; Bohara, V.A.; Srivastava, A. On the optimization of integrated terrestrial-air-underwater architecture using optical wireless communication for future 6G network. *IEEE Photonics J.* **2022**, *14*, 1–12.
- 3. Zhang, Z.; Xiao, Y.; Ma, Z.; Xiao, M.; Ding, Z.; Lei, X.; Karagiannidis, G.K.; Fan, P. 6G wireless networks: Vision, requirements, architecture, and key technologies. *IEEE Veh. Technol. Mag.* **2019**, *14*, 28–41.
- 4. Li, X.; Gui, L.; Xia, Y.; Lang, L. Demonstration of a real-time UWOC system using a bandwidth limited LED based on hardware and software equalization. *J. Light. Technol.* **2023**, *41*, 4979–4988.
- 5. Kaushal, H.; Kaddoum, G. Underwater optical wireless communication. IEEE Access 2016, 4, 1518–1547.
- 6. Xu, J. Underwater wireless optical communication: Why, what, and how? [Invited]. Chin. Opt. Lett. 2019, 17, 34–43.
- 7. Diamant, R.; Campagnaro, F.; de Filippo de Grazia, M.; Casari, P.; Testolin, A.; Sanjuan Calzado, V.; Zorzi, M. On the relationship between the underwater acoustic and optical channels. *IEEE Trans. Wirel. Commun.* **2017**, *16*, 8037–8051.
- 8. Zeng, Z.; Fu, S.; Zhang, H.; Dong, Y.; Cheng, J. A survey of underwater optical wireless communications. *IEEE Commun. Surv. Tutor.* **2017**, *19*, 204–238.
- 9. Li, Y.; Yin, H.; Ji, X.; Wu, B. Design and implementation of underwater wireless optical communication system with high-speed and full-duplex using blue/green light. In Proceedings of the International Conference on Communication Software and Networks (ICCSN), Chengdu, China, 6–9 July 2018; pp. 99–103.
- 10. Elamassie, M.; Miramirkhani, F.; Uysal, M. Performance characterization of underwater visible light communication. *IEEE Trans. Commun.* **2019**, *67*, 543–552.
- 11. Wang, J.; Chen, C.; Deng, B.; Wang, Z.; Liu, M.; Fu, H.Y. Enhancing underwater VLC with spatial division transmission and pairwise coding. *Opt. Express* **2023**, *31*, 16812–16832.
- 12. Jiang, H.; Qiu, H.; He, N.; Popoola, W.; Ahmad, Z.; Rajbhandari, S. Ergodic capacity and error performance of spatial diversity UWOC systems over generalized gamma turbulence channels. *Opt. Commun.* **2022**, *505*, 127476.
- 13. Sabeer, S.; Hassib, M.D.; Jameel, Z.N. A review: Error correcting codes for efficient underwater optical communication MIMO system. In Proceedings of the International Conference on Communication and Information Technologies (IICCIT), Basrah, Iraq, 7–8 September 2022; pp. 13–19.
- 14. Kurnia, R.; et al. Hamming coding for multi-relay cooperative quantize and forward networks. In Proceedings of the IEEE Region 10 Symposium (TENSYMP), Bali, Indonesia, 9–11 May 2016; pp. 321–325.
- 15. Cai, Y.; Wang, W.; Qian, W.; Xing, J.; Tao, K.; Yin, J.; Zhang, S.; Lei, M.; Sun, E.; Chien, H.C.; et al. FPGA investigation on error-flare performance of a concatenated staircase and Hamming FEC code for 400G inter-data center interconnect. *J. Light. Technol.* **2019**, 37, 188–195.

16. Sybis, M.; Wesolowski, K.; Jayasinghe, K.; Venkatasubramanian, V.; Vukadinovic, V. Channel coding for ultra-reliable low-latency communication in 5G systems. In Proceedings of the IEEE 84th Vehicular Technology Conference (VTC-Fall), Montréal, QC, Canada, 18–21 September 2016; pp. 1–5.

- 17. Rani, M.; Singal, P. An efficient IDMA-OFDM underwater wireless communication with Reed Solomon and Hamming code. *J. Opt.* **2022**, *51*, 456–466.
- 18. Deng, B.; Wang, J.; Wang, Z.; Qasem, Z.A.H.; Li, Q.; Tang, X.; Chen, C.; Fu, H.Y. Polarization multiplexing based UOWC systems under bubble turbulence. *J. Light. Technol.* **2023**, *41*, 5588–5598.
- 19. He, J.; Xu, L.; He, J.; Xiao, Y. Performance comparison of different rotated QAM based DMT schemes in underwater optical wireless communication. *J. Light. Technol.* **2023**, *41*, 610–617.
- 20. Huang, X.; Chen, S.; Wang, Z.; Shi, J.; Wang, Y.; Xiao, J.; Chi, N. 2.0-Gb/s visible light link based on adaptive bit allocation OFDM of a single phosphorescent white LED. *IEEE Photonics J.* 2015, 7, 1–8.
- 21. Zhang, Z.; Lai, Y.; Lv, J.; Liu, P.; Teng, D.; Wang, G.; Liu, L. Over 700 MHz –3 dB bandwidth UOWC system based on blue HV-LED with T-bridge pre-Equalizer. *IEEE Photonics J.* **2019**, *11*, 1–12.
- 22. Zhao, Y.; Chi, N. Partial pruning strategy for a dual-branch multilayer perceptron-based post-equalizer in underwater visible light communication systems. *Opt. Express* **2020**, *28*, 15562–15572.
- 23. Chen, C.; Nie, Y.; Liu, M.; Du, Y.; Liu, R.; Wei, Z.; Fu, H.Y.; Zhu, B. Digital pre-equalization for OFDM-based VLC systems: Centralized or distributed? *IEEE Photonics Technol. Lett.* **2021**, 33, 1081–1084.
- 24. Zhou, X.; Urata, R.; Liu, H. Beyond 1 Tb/s intra-data center interconnect technology: IM-DD or coherent? *J. Light. Technol.* **2020**, 38, 475–484.
- 25. Popoola, W.O.; Ghassemlooy, Z. BPSK subcarrier intensity modulated free-space optical communications in atmospheric turbulence. *J. Light. Technol.* **2009**, 27, 967–973.
- 26. Bekkali, A.; Naila, C.B.; Kazaura, K.; Wakamori, K.; Matsumoto, M. Transmission analysis of OFDM-based wireless services over turbulent radio-on-FSO links modeled by Gamma–Gamma distribution. *IEEE Photonics J.* **2010**, *2*, 510–520.
- 27. Hessien, S.; Tokgöz, S.C.; Anous, N.; Boyacı, A.; Abdallah, M.; Qaraqe, K.A. Experimental evaluation of OFDM-based underwater visible light communication system. *IEEE Photonics J.* **2018**, *10*, 1–13.
- 28. Jiang, H.; Qiu, H.; He, N.; Popoola, W.; Ahmad, Z.; Rajbhandari, S. Performance of spatial diversity DCO-OFDM in a weak turbulence underwater visible light communication channel. *J. Light. Technol.* **2020**, *38*, 2271–2277.
- 29. Hong, Y.; Wu, T.; Chen, L.K. On the performance of adaptive MIMO-OFDM indoor visible light communications. *IEEE Photonics Technol. Lett.* **2016**, *28*, 907–910.
- 30. Başar, E.; Panayırcı, E. Optical OFDM with index modulation for visible light communications. In Proceedings of the International Workshop on Optical Wireless Communications (IWOW), Istanbul, Turkey, 7–8 September 2015; pp. 11–15.
- 31. Jaradat, A.M.; Hamamreh, J.M.; Arslan, H. OFDM with subcarrier number modulation. *IEEE Wirel. Commun. Lett.* **2018**, 7 914–917
- Wen, M.; Li, J.; Dang, S.; Li, Q.; Mumtaz, S.; Arslan, H. Joint-mapping orthogonal frequency division multiplexing with subcarrier number modulation. *IEEE Trans. Commun.* 2021, 69, 4306–4318.
- 33. Chen, J.; Deng, B.; Chen, C.; Liu, M.; Fu, H.Y.; Haas, H. Efficient capacity enhancement using OFDM with interleaved subcarrier number modulation in bandlimited UOWC systems. *Opt. Express* **2023**, *31*, 30723–30734.
- 34. Chun, H.; Gomez, A.; Faulkner, G.; O'Brien, D. A spectrally efficient equalization technique for optical sources with direct modulation. *Opt. Lett.* **2018**, *43*, 2708–2711.
- 35. Brennan, D. Linear diversity combining techniques. *Proc. IEEE* 2003, 91, 331–356.
- 36. Chen, C.; Zhong, W.D.; Yang, H.; Zhang, S.; Du, P. Reduction of SINR fluctuation in indoor multi-cell VLC systems using optimized angle diversity receiver. *J. Light. Technol.* **2018**, *36*, 3603–3610.
- 37. Chen, C.; Zhong, W.D.; Wu, D.; Ghassemlooy, Z. Wide-FOV and high-gain imaging angle diversity receiver for indoor SDM-VLC systems. *IEEE Photon. Technol. Lett.* **2016**, *28*, 2078–2081.
- 38. Qian, Y.; Chen, C.; Du, P.; Liu, M. Hybrid space division multiple access and quasi-orthogonal multiple access for multi-user underwater visible light communication. *IEEE Photonics J.* **2023**, *15*, 7303507.
- 39. Yin, H.; Alamouti, S. OFDMA: A broadband wireless access technology. In Proceedings of the IEEE Sarnoff Symposium, Princeton, NJ, USA, 27–28 March 2006; pp. 1–4.
- 40. Nie, Y.; Chen, J.; Wen, W.; Liu, M.; Deng, X.; Chen, C. Orthogonal subblock division multiple access for OFDM-IM-based multi-user VLC systems. *Photonics* **2022**, *9*, 373.

**Disclaimer/Publisher's Note:** The statements, opinions and data contained in all publications are solely those of the individual author(s) and contributor(s) and not of MDPI and/or the editor(s). MDPI and/or the editor(s) disclaim responsibility for any injury to people or property resulting from any ideas, methods, instructions or products referred to in the content.